Journal of Nondestructive Evaluation (2021) 40:65
https://doi.org/10.1007/s10921-021-00797-3

Muon Tomography of the Interior of a Reinforced Concrete Block: First Experimental Proof of Concept

Ernst Niederleithinger[1] · Simon Gardner[2] · Thomas Kind[1] · Ralf Kaiser[2,3] · Marcel Grunwald[1] · Guangliang Yang[2,3] · Bernhard Redmer[1] · Anja Waske[1] · Frank Mielentz[1] · Ute Effner[1] · Christian Köpp[1] · Anthony Clarkson[2,3] · Francis Thomson[2,3] · Matthew Ryan[4] · David Mahon[2]

Received: 7 August 2020 / Accepted: 4 July 2021 / Published online: 24 July 2021

Abstract
Quality assurance and condition assessment of concrete structures is an important topic world-wide due to the aging infrastructure and increasing traffic demands. Common topics include, but are not limited to, localisation of rebar or tendon ducts, geometrical irregularities, cracks, voids, honeycombing or other flaws. Non-destructive techniques such as ultrasound or radar have found regular, successful practical application but sometimes suffer from limited resolution and accuracy, imaging artefacts or restrictions in detecting certain features. Until the 1980s X-ray transmission was used in case of special demands and showed a much better resolution than other NDT techniques. However, due to safety concerns and cost issues, this method is almost never used anymore. Muon tomography has received much attention recently. Novel detectors for cosmic muons and tomographic imaging algorithms have opened up new fields of application, such as the investigation of freight containers. Muon imaging also has the potential to fill some of the gaps currently existing in concrete NDT. As a first step towards practical use and as a proof of concept we used an existing system to image the interior of a reference reinforced 600 kg concrete block. Even with a yet not optimized setup for this kind of investigation, the muon imaging results are at least of similar quality compared to ultrasonic and radar imaging, potentially even better. The data acquisition takes more time and signals contain more noise, but the images allowed to detect the same important features that are visible in conventional high energy X-ray tomography. In our experiment, we have shown that muon imaging has potential for concrete inspection. The next steps include the development of mobile detectors and optimising acquisition and imaging parameters.

Keywords Muon tomography · Non-destructive testing · Reinforced concrete · Ultrasound · Radar · X-ray

1 Introduction

The continuous availability of the European road transport network is one of the essential prerequisites for mobility and economic growth in the EU and world-wide. EU road infrastructure is getting older and suffers from aging issues with a large part of it already approaching the end of its life. According to the European Union Road Federation, the network had a length of 5.5 million km and a value of 8000 billion Euros in 2018, the latter declining [1]. In Germany, 10% of the bridges (bridge deck area considered) under federal administration were rated with a condition "less than sufficient" [2]. In France, about 25,000 bridges are prone to structural health issues which affect both safety and accessibility [3]. They are subject to serious fatigue problems, due to the increase of freight volumes (and traffic) with ever greater overall vehicle weights. Bridges and roads allow individual mobility and the supply of private households and the economy, but their aging and upcoming fatigue problems lead to progressive degradation of bridge structures and thus to safety and reliability problems. These effects are further intensified by technological developments in heavy goods vehicle traffic (e.g. road trains, platooning

✉ Ernst Niederleithinger
ernst.niederleithinger@bam.de

[1] Bundesanstalt für Materialforschung und -prüfung (BAM), Berlin, Germany

[2] School of Physics & Astronomy, University of Glasgow, University Avenue, Glasgow G12 8QQ, UK

[3] Lynkeos Technology Ltd., University of Glasgow, No 11 The Square, Glasgow G12 8QQ, UK

[4] National Nuclear Laboratory, Central Laboratory, Sellafield, Seascale, Cumbria CA20 1PG, UK

etc.). Damage to structures that is usually only detected at a late stage, can have far-reaching consequences for traffic. In the worst case, the total failure of a structure can lead to the complete inaccessibility of entire road sections in the traffic network, as illustrated by the collapse of the Polcevera Viaduct (aka Morandi Bridge) in Genoa in August 2018, leading to multiple deaths and resulting in a significant loss of gross domestic product. Traditional approaches for assessing the condition of transport infrastructure are based on structural inspections at fixed or adjustable time intervals. They are inadequate for an efficient inspection of the transport infrastructure assets, which after all amount to about 40% of the total European assets [1]. Only an efficient inspection, preferably permanently under flowing traffic, will give infrastructure owners and managers the right picture to prioritize their maintenance operations.

There are already a number of Non-Destructive Testing (NDT) methods that provide engineers with tools to inspect aging infrastructure [3, 5–8]. Standard technologies for structure assessments are ultrasonic methods and ground penetrating radar. For specific tests, e.g. reference measurements with very high resolution, X-ray radiography is also used. However, all of these techniques have their limitations. Ground penetrating radar is a very rapid and effective inspection method and is very sensitive for metal detection, but in concrete constructions the penetration depth and resolution of ground penetrating radar depend on the frequency of the radar used: low frequencies can penetrate up to 1.5 m with resolutions of several cm and high frequencies can reach resolutions of several mm but the penetration depth is limited to about 40 cm. Ultrasonic echo instruments show greater penetration depths (around 1 m in commercial applications) but have a resolution of at best 1 cm. In addition, it is often not possible to inspect beyond the first reinforcement layers due to reflections. Ultrasonic echo methods are excellent to detect voids, cracks or delaminations, but cannot image features behind these obstacles. X-ray radiography (including variants such as X-ray tomography and laminography) can provide images with excellent resolution. Depending on the radiation energy, the penetrated thickness of a concrete structure can be up to 1 m with a spatial resolution of a few mm. However, when using X-ray radiography, attention must always be paid to compliance with the radiation protection regulations. In practice this often means that X-ray radiography cannot be applied.

Muon tomography, a purely passive technique using natural cosmic background radiation as a source, has the potential to overcome some of these issues [9]. Showers of high energy particles, including muons, are constantly created by collisions between cosmic rays and the upper atmosphere. The muons from these showers are highly penetrative and can pass through tens and hundreds of meters of rock before coming to rest and decaying. As cosmic muons are a naturally occurring radiation there are no costs or energy requirements in generating them, and because no additional radiation is generated there is no safety concern. It is a passive imaging system. There are two types of muon imaging techniques. The first is muon absorption imaging (or muon radiography), and the second is muon multiple scattering imaging (or muon tomography). While muon radiography uses one detector (or a set of detectors on the same plane) to detect muons after passing the object of interest, muon tomography uses two detectors (or two sets of detectors on different planes) to detect the muons before and after passing through the object of interest. The latter allows volumetric reconstruction of the object's scattering properties, resulting in high resolution 3D images [10].

The absorption of naturally occurring cosmic-ray muons was first used to investigate complex structures over 60 years ago by British physicist George, when he determined the weight of ice above a mining tunnel in Australia [11]. Imaging the interior of a volcano by muography was shown in 2001 [12]. Fifteen years ago, researchers at Los Alamos National Laboratory demonstrated that the Coulomb-scattering of the muon could be exploited to identify high-density, high-atomic number (Z) material within large, shielded transport containers [13, 14]. Since this discovery, the field of non-destructive testing using cosmic ray muography has developed and, in recent years, has experienced an exponential growth with more than 40 research groups and projects active in over 20 countries throughout the world. In 2017 the topic received great attention with the publication of the high-profile measurements from within the great pyramid of Khufu in Egypt that indicated the presence of a previously unknown chamber [15]. In recent years, half a dozen companies have formed to commercialise muography imaging technology for a variety of different applications including nuclear contraband detection for national security, brownfield mineral exploration and nuclear waste characterisation. Recently, an experiment using muography for the detection of animal burrows in river embankments was reported [16].

The application of muon tomography to nuclear waste containers includes the investigation of objects or voids in concrete as this is used for stabilizing and shielding waste objects inside the containers. However, in the experiments published so far, the size of the detected objects (several cm) is larger than what would be required for reinforced concrete in civil engineering. The diameter of rebar is typically between 8 and 28 mm. The idea to use muon tomography to inspect civil engineering concrete structures is e. g. reported by Durham et al. in 2016 [18]. The same paper describes a successful experiment mapping section of a concrete panel with different thicknesses. However, there is no practical demand for thickness measurements on real constructions if both sides are accessible. The idea of using muon tomography as a tool for the inspection of interior

features of reinforced concrete structures including a concept for developing a suitable mobile detecting system was submitted to the EC research program Horizon 2020 in early 2019 by the authors. Civil engineering, especially bridge inspection, was also highlighted as a key future application in an overview article by one of the authors in 2019 [9]. The same idea was developed by another research group and successfully explored by simulations [19]. Other similar applications reported have been limited to simulations or conceptual designs due to the lack of suitable detectors [20, 21].

As a proof of concept experiment, muon tomography of a reference reinforced concrete block produced by BAM (German Federal Institute for Materials Research and Testing) was carried out at the University of Glasgow in September 2019 using a detector system originally developed to examine radioactive waste containers. To our knowledge, this is the first ever experiment of this kind. The results have been compared to several state-of-the-art techniques for concrete NDT at BAM. We have chosen the ultrasonic echo and radar echo techniques as the most used, state-of-the-art methods for non-destructive investigation of the internal geometry of concrete structures. X-ray laminography was performed as a reference. Note, that we are aiming for a qualitative evaluation only, serving as a prof, that further developments and investments in this technology are justified.

The paper is organized as follows: in the Sect. 2, the reference concrete block is introduced as well as the various methods and devices used for examination, including techniques for data processing and imaging. In Sect. 3 the images produced by the various techniques are shown and compared for three different horizontal cross sections of the reference block. In Sect. 4 the advantages and limitations are compared. Section 5 finalise this paper.

2 Materials and Methods

2.1 The Reference Concrete Block "Radarplatte"

The reference concrete block "Radarplatte" (radar slab) was produced for training purposes. In its volume of 1.2 m × 1.2 m × 0.2 m four different targets were placed, which are typical for reinforced concrete structures (Fig. 1). Near to the top and the back, reinforcement bar mats were placed, each covering just about 50% of the area and overlapping on about 25% of the area. Depth of rebar is between about 30 mm (bottom) and about 50 mm (top). The mat at the top has a mesh size of 150 mm, diameter of 10 mm, and the one on the bottom mesh of 100 mm, diameter of 6 mm. In between these two-reinforcement bar mats, an empty tendon duct with an outer diameter of 65 mm and a concrete cover of 90 mm was placed. Finally, a Styrofoam block of 600 mm × 300 mm × 50 mm was inserted at the bottom to simulate a flaw at the backwall of the block.

2.2 Muon Tomography

Muon tomography is a technique, which is used to reconstruct 3D density maps of volumes using the Coulomb scattering of muons [9, 10]. By measuring the tracks of muons as they enter and exit the volume, an estimate of the average magnitude of scattering occurring in discrete volume elements can be calculated. Due to their high average energy of several GeV, i.e. 10,000 times higher than the typical X-ray energy, and due to the way muons interact with matter, they are highly penetrating and can pass through hundreds of meters of rock (or concrete).

The primary advantages of using muon tomography over other methods are penetration depth and the fact that it is entirely passive and non-destructive method. The comparatively long time it takes to make a measurement using cosmic-ray muons, can be considered its main detractor; millions of muons are required to create a high-resolution image and the flux of muons at sea level is around 170 Hz/m^2. This means that in practice data needs to be collected continuously for days or even weeks. The flux of muons also has a strong angular dependence, characterised by $\cos^2\theta$ to the vertical, which leads to a better imaging resolution in the horizontal plane than in the vertical direction.

Note, that the term tomography is used differently in muon imaging and X-ray radiography related literature. In NDT standards, including those for X-ray imaging, tomography refers to imaging methods using 360° ray coverage, generated by rotating the object or the source/detector setup. The correct term for imaging planar objects with limited ray coverage (access just from two sides of the object) is laminography. However, to be consistent with the respective literature we are staying with the term tomography for the muon imaging method used in this research.

The Lynkeos Muon Imaging System (MIS), used for the investigation of the "Radarplatte", consists of 4 detector modules each containing 2 orthogonal layers of scintillating fibres read out with 64-channel multi-anode photomultipliers. From the fibre hits in each module a space point of the muon hit can be determined (Fig. 2, Table 1) [13]. Two modules placed above the volume are used to reconstruct the incident muon tracks and two below for the outgoing, scattered tracks.

The active area of the MIS modules is 1 m by 1 m. The horizontal resolution of the MIS is limited by the 2 mm diameter of the scintillating fibres used in the detectors; these are triangularly packed in two sublayers allowing an effective resolution of less than 2 mm where muons pass through neighbouring fibres. The vertical resolution of the reconstructed image is of the order of 4 cm due to the

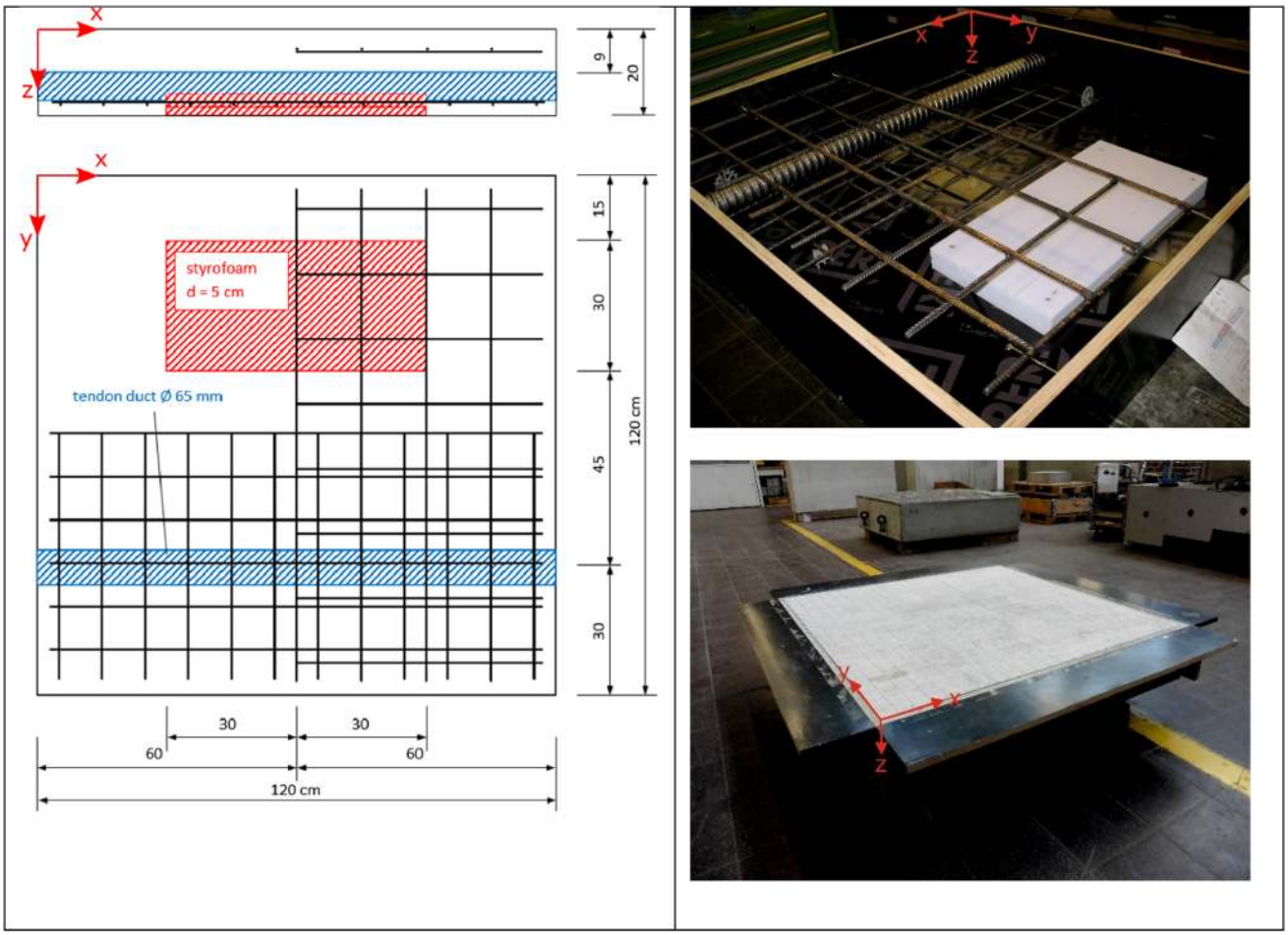

Fig. 1 The reference concrete block "Radarplatte". Left: Design cross-section and view from above. Right: Pictures before and after concreting

angular acceptance of the detector being limited to near vertical tracks. The most important parameters are compiled in Table 1.

The first two algorithms that were developed and published for the reconstruction of muon tomography data are known as POCA (point of closest approach) and MLEM (maximum likelihood expectation maximization) [20]. They are well known and widely used. A detailed overview of the different algorithms in use has been published by some of the authors [10]. The image reconstruction for the muon tomography data used in this paper is the MLEM algorithm. A detailed description of the MLEM algorithm can be found in a paper published by the Los Alamos group [23]. As part of the reconstruction, the volume between the top and bottom detectors is divided into voxels. The reconstructed value attributed to each voxel is calculated based by MLEM on the average measured scatter of the set of muons which pass through the voxel. The voxel value is expected to increase with the density of the volume it relates to.

In total 23 million muon tracks were used to reconstruct the tomographic image of the concrete sample. These muons were detected during the continuous running of the MIS for 1203 h between 23rd September and 12th November 2019.

2.3 Radar

Radar is a non-destructive testing tool for the investigation of Civil Engineering structures and is based on the transmission and reception of electromagnetic waves [24–27]. The received signal gives information about the internal structure of an investigated object by reflecting the transmitted electromagnetic wave back from objects which are conductive like metals or have different dielectric properties like concrete and air. The distance and position of objects can be derived from the received signal and material properties by analysing the size and shape of the received signal. The equipment for radar is designed for using different broadband antennas with a relative bandwidth of about 100%. The typical centre frequency of these antennas, which are applied for the investigation of reinforced concrete buildings, lies in a range of 1 to 3 GHz.

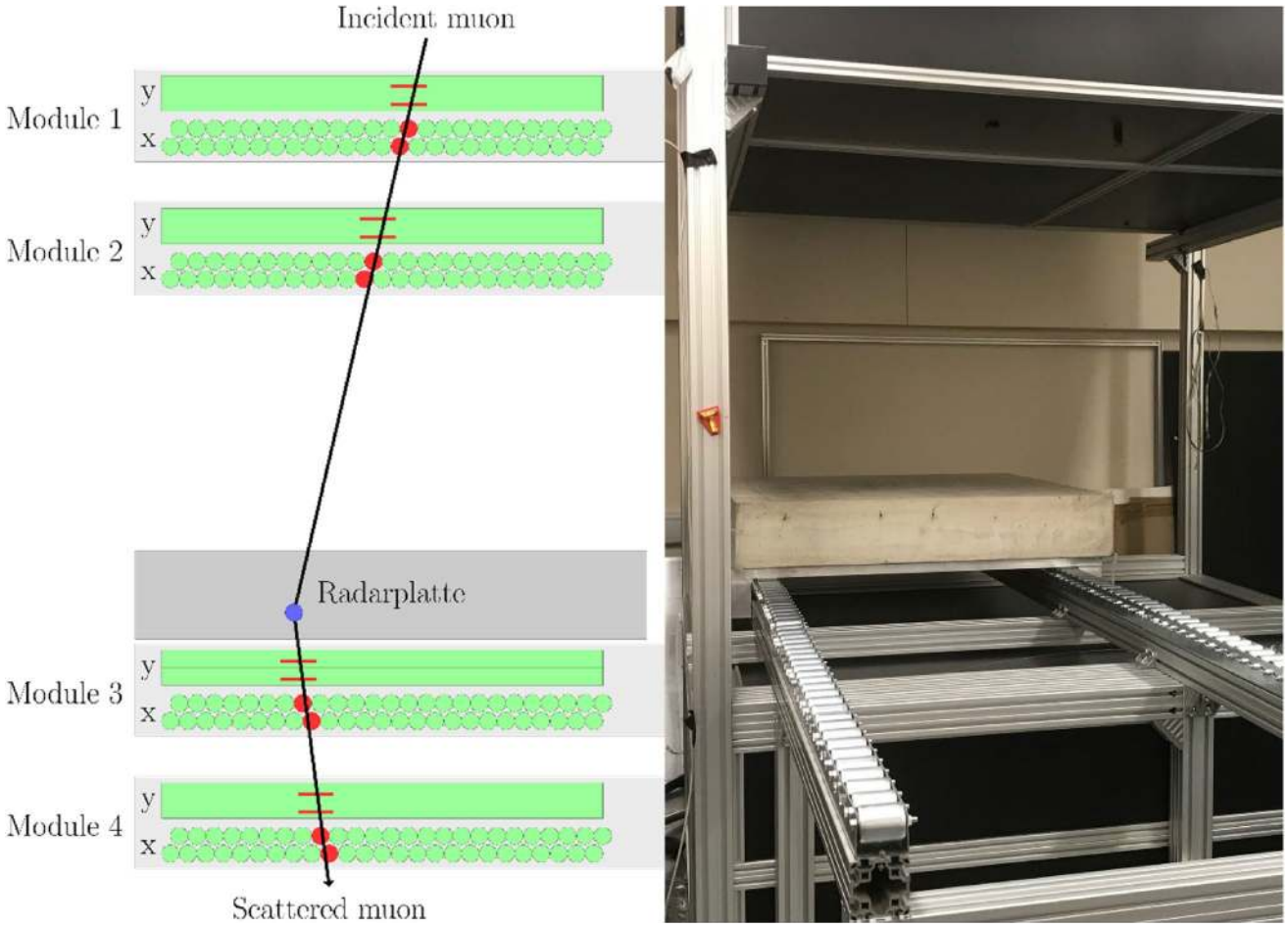

Fig. 2 Muon Imaging. Left: principle of muon tomography. Two detectors above and two detectors below the object were used to trace muon flight paths and scattering, Right: the "Radarplatte" test object inside the Lynkeos Muon Imaging System (MIS)

Table 1 Experimental parameters for muon tomography

Source	Cosmic ray muons (1 to 100 GeV)
Detector	Lynkeos Muon Imaging System (MIS) 1024 × 1024 Fibres (Resolution < 2 mm) Exposure time = 1203 h Trigger rate = 11 Hz
Reconstruction	Voxel size 3.4 mm × 3.4 mm × 10 mm Volume size 300 × 300 × 178 Voxels (1060 × 1060 × 1780 mm^3)

The penetration depth decreases with higher frequencies and the resolution increases simultaneously.

The radar data were collected by guiding a radar antenna manually along parallel lines, where the distance between lines was 5 cm. Lines were parallel to the sides of the "Radarplatte" (Fig. 3). A distance wheel encoder was connected to the antenna to collect A-scans (amplitude scan, recorded time series for a specific transmitter–receiver configuration) every 2.5 mm along the line. Data were acquired both in x- and y-direction.

An antenna with a centre frequency of 2 GHz was used and connected to a radar control unit (GSSI SIR3000, Fig. 3). The collected data were analysed using the proprietary software of the manufacturer. The main processing steps included the application of a travel time dependent gain, 2D reconstruction by Kirchhoff migration and the calculation of the envelope function by Hilbert transform. As the response of rebar is highly dependent on the antenna polarization, all processed profiles (x- and y-direction) were assembled to a three-dimensional data cube by adding the respective amplitudes for the two measurements for each voxel. This allows the visualization of rebar independent of its orientation. The travel time axis of the three-dimensional data cube was transformed to a depth axis by using a constant wave propagation speed.

In general, a characterization of objects is possible with radar (and as well with ultrasound) by evaluating the phase information in the reflected signals, but this involves

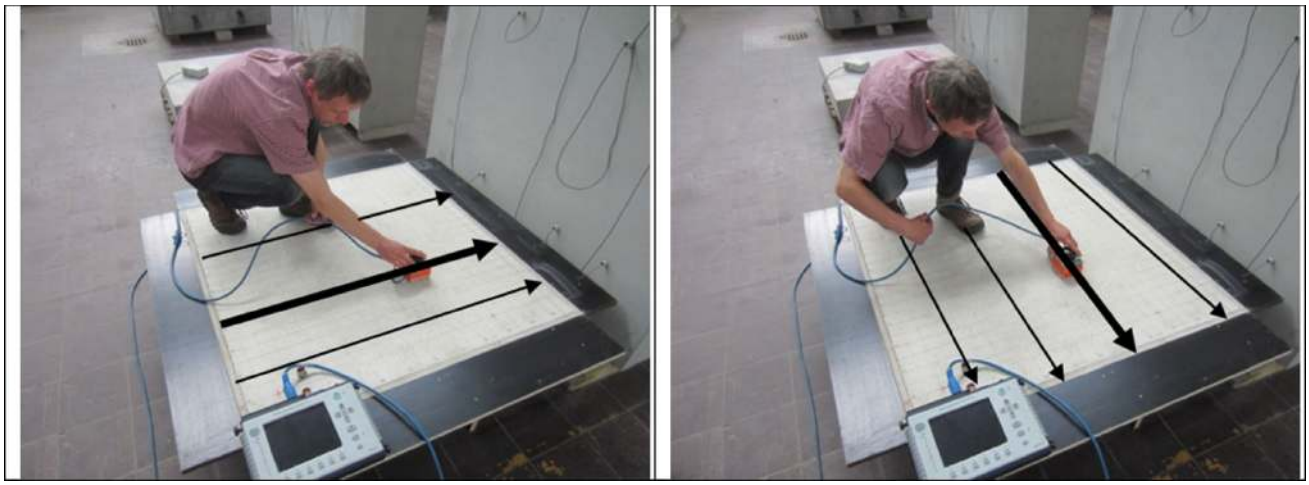

Fig. 3 Radar data acquisition and the orientation of the two sets of measurement lines on top of the "Radarplatte"

additional non-standard processing steps and has not been used here.

Two dimensional projections at three depths were generated. The depths were 5 cm, 12 cm and 17 cm. Each depth slice was averaged over 1 cm in z-direction.

2.4 Ultrasound

Ultrasonic echo measurements have been established for the investigation of concrete constructions for about 25 years. Point contact shear wave transducers, without the need of a coupling agent, were introduced into practical application in the mid-1990s and are now almost exclusively used in the testing of concrete components. Today's commercial devices consist of two to sixteen arrays of three to twelve coupled transducers. The frequency range is in between 40 and 60 kHz (3 dB attenuation), leading to a resolution in the centimeter-range. Reflections are recorded from elastic impedance contrasts within the object (e.g. concrete-steel, concrete-air) and from its boundaries. At interfaces to air, the energy is almost totally reflected, shadowing all features behind such interfaces. This means that ultrasonic echo techniques cannot image features behind e.g. delamination. Aggregates and larger pores are causing scattering of ultrasonic waves, leading to an inherent level of structural noise. Depth of penetration is limited to values around 1 m, depending on the degree of reinforcement, porosity, aggregate size, and other factors. The method is mainly used for thickness measurement, geometry evaluation, detection of larger rebar, tendon ducts, voids, cracks and delaminations. The state of the art is described e.g. in [28–30].

The ultrasonic data were collected using an automated scanning system (Fig. 4) developed by BAM. A transducer array ("ultrasonic probe" in Fig. 4) with 12 shear wave point contact transducers, each for transmitting and receiving, was

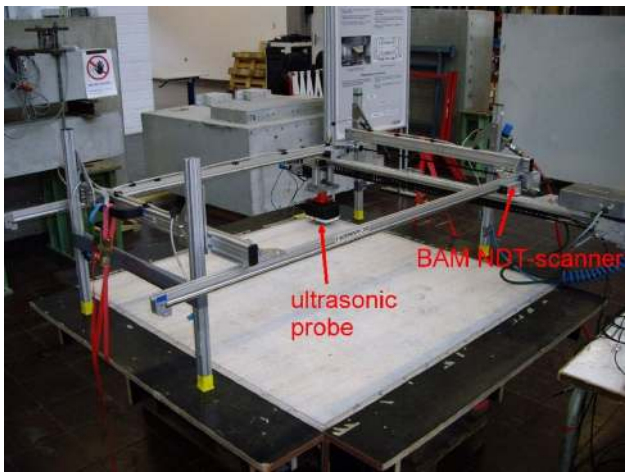

Fig. 4 BAM NDT scanner with ultrasonic shear wave probe (Acsys M2503) mounted on the "Radarplatte"

used. The probe was connected to an ultrasonic setup based on a custom-made pulse generator and commercial data acquisition equipment. Two data sets were collected on a 2 cm by 2 cm grid using different orientations of the probe (x- and y-polarization). The data sets were processed and imaged using the software InterSAFT developed by University of Kassel [31]. The most important parameters are shown in Table 2. Other than with radar, the resulting data volumes for x- and y-direction were kept separate. In the results section, the data set showing the greater response to the features in question, is displayed.

2.5 X-ray Laminography

While X-ray computed tomography (CT) has been widely used as a common non-destructive imaging technique, it is

Table 2 experimental parameters for ultrasound

Probe	Acsys M2503
Data Acquisition	BAM proprietary setup using NI components, BAM NDT scanner
Pulse center frequency	50 kHz
Sample rate	1 MHz
Samples	1000
Point (A-scan) distance	2 cm by 2 cm
Number of A-scans	51×51 (10 cm offset to the edges)
Polarization	x- and y-direction
Reconstruction	SAFT (Software InterSAFT)

not well-suited to visualize internal structures of large and flat objects. This is because CT requires a full rotation of the object and the object must fit in the field-of-view of the digital X-ray detector. Laminography or tomosynthesis are applied on laterally extended planar objects with large aspect ratios for example pipelines, large concrete samples, and rotors of wind power plants, where the 360° image acquisition around the object is not physically possible.

In classical laminography, which is based on a relative motion of the X-ray source, the detector and the object can be set up in different geometrical arrangements. The X-ray source and the detector are either moved synchronously on circular paths around the object, a so-called rotational laminography, or are simply moved in opposite directions in the case of translational laminography.

Planar tomography (PT) as a special case of coplanar translation laminography was used to investigate the concrete plates using the HEXYTech equipment of BAM (Fig. 5). The radiation source (X-ray tube, gamma source, accelerator) and detector (e.g. matrix detector) are moved synchronized and parallel to the object, whereas the object remains stationary. The detector size is smaller than the "Radarplatte". Thus, the detector had been moved several times, forming six overlapping frames in a 3 by 2 array). For each frame, the object is irradiated by X-rays from various source positions (usually several hundred) and the radiation that penetrates the object is recorded by the detector. The digitally stored projections contain 3-dimensional information about the object. A 3D volume data set of the studied object is reconstructed from the projections by a filtered backpropagation algorithm (FBP) that is adapted to the specific geometry of the laminography arrangements. In the volume data set of the concrete plate, different features can be detected, e.g. reinforcement, concrete matrix, cracks, and air inclusions [28]. Typically, X-ray laminography data is not free of artefacts that result from irregular illumination or the high pass filter used by the reconstruction algorithm to enhance the edges in the projection data. These artefacts may complicate the quantitative analysis of the internal features of the object.

The experimental parameters of the planar tomography of the "Radarplatte" are described in Table 3. The pixel resolution of the digital detector was 400 µm. The total number of single projections was approx. 7300.

3 Experimental Results

The experimental results have been acquired and processed as described in the previous section, resulting in 3D voxel datasets of the investigated volume. The voxel datasets have been geometrically referenced to the upper main surface of the "Radarplatte" (z = 0 m). The x and y axis are along the longer edges (Fig. 1). To evaluate and compare the results of

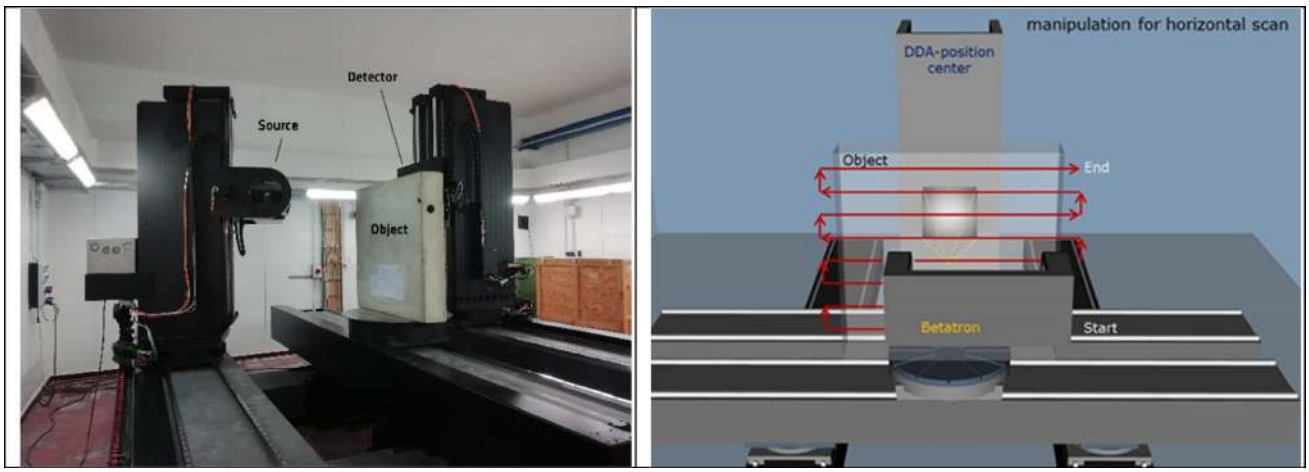

Fig. 5 Left: HEXYTech-equipment for X-ray laminography of large and thick-walled test object. Right: sketch of the horizontal scanning procedure. For each frame position the source and detector move synchronously along the marked paths (red) relative to the object movement and several hundred projections are recorded for each (horizontal) path

Table 3 Experimental parameters for X-ray planar tomography

Source	Betatron JME 7.5 MeV, focus spot size = 0.3 mm • 3 mm
Detector	Perkin Elmer XRD 1024 × 1024 Pixel (Resolution 400 µm) Exposure time: 1000 ms Number of frames: 6, arranged in 3 by 2 array
Reconstruction	Voxel size: 0.5 mm × 0.5 mm × 1.5 mm Volume size: 2460 × 1170 × 200 Voxels (1230 × 585 × 300 mm^3)

the investigations, three depth sections parallel to the upper surface have been extracted at depths of 5 cm, 12 cm, and 17 cm below the upper surface.

Note, that these depth sections are not necessarily produced by the respective values at the precise depth but may be averaged over a certain depth interval. This is a usual procedure for ultrasonic and radar images acquired on concrete to smooth the structural noise caused by the inherent inhomogeneous nature of concrete. Here, muon tomography is an exception where only single slices of the reconstructed volume are shown. Some of the datasets are limited to certain parts of the object due to experimental limitations of the devices used. X-ray tomography misses 10 cm of the upper part of the block (y = 110 to 120 cm). The muon tomography is currently limited to 1 m by 1 m and misses a small part of the left top corner, and a larger part of the bottom right corner. In addition, the object was inserted into the muon detection system with an offset of the edges of 0.6 degrees, which was not corrected in the imaging process. These limitations can be overcome by optimizing the setup.

The uppermost of the three depth levels discussed here, intersects with the upper reinforcement mesh (Fig. 6a). Muon tomography (Fig. 6b) shows all rebars clearly, proving a horizontal resolution of at least about 1 cm of this technique. Some of the features at larger depth show up slightly (tendon duct and Styrofoam plate) as bright shadows, which is typical for experiments of the transmission tomography type. Shadow artefacts from the support structure of the sample table appear as dark vertical lines at x between 10 and 20 cm and above x = 105 cm. Radar (Fig. 6c) shows all rebars clearly, but the signatures are wider than the actual bars (about 20 mm in this visualization). Ultrasound (Fig. 6d) is not able to image the reinforcement in this case as it is beyond the resolution limit for the setup used here. X-ray laminography (Fig. 6e) shows the clearest picture of all presented technologies. Shadows from deeper features and boundary effects are similar to the ones seen in muon tomography. Interestingly, the images of the reinforcement grid show non-equidistant spacing and other distortions for all applicable technologies. These deviations from the design drawings were visible as well in a detailed photograph (Fig. 6f) of the reinforcement grid before concreting, thus not being associated to distortions of the images but to the actual internal geometry of the object under investigation.

The second depth level (12 cm) intersects with the center of the tendon duct (Fig. 7a). All technologies are able to image this feature, alas, with different clarity and level of detail. While X-ray laminography (Fig. 7e) shows even the undulations of the corrugated pipe, all other methods images are more or less straight shaped and show a significant level of noise. Radar (Fig. 7c) shows artefacts from the reinforcement layer above, which is typical for echo techniques. Muon tomography shows the tendon duct with a clarity comparable to radar and ultrasound. As in X-ray laminography, artefacts from features above and below are present.

The third depth level studied intersects with the lower reinforcement and the Styrofoam block (Fig. 8a). The Styrofoam block is imaged by all techniques, while the reinforcement is missed by ultrasound (Fig. 8d) for the same reasons as the upper reinforcement. The radar image (Fig. 8c) is partially distorted by artefacts caused by the features above this depth level. These features show up in the muon tomography (Fig. 8b) and X-ray laminography (Fig. 8e) images as well, but with lesser effect on the image of the objects, which are actually at this depth level. Radar and X-ray-laminography pick up the irregular spacing between the two y-oriented rebar at the left edge, which is visible in the close-up photograph (Fig. 8e). In the muon tomography image this is hard to verify due to an imaging artefact. Note, that the rebar diameter of the lower mat is just 6 mm, verifying the potential of muon tomography for sub-cm resolution.

4 Discussion

The muon tomography images, acquired with a setup which is not yet optimized for concrete inspection, have shown that high density and low density features in concrete objects can be imaged by this emerging technology and be distinguished without further data processing (low density/air: bright, high density/steel: dark). The resolution of muon tomography might exceed the one of ultrasound and radar, at least for the scenario investigated here. Some artefacts are present in the images. Some (e.g. the shadows of objects above and below the depth level under consideration) are due to two inherent limitations of the technology: first, tomographic reconstruction algorithms may produce artefacts and are"smearing" anomalies in case of limited angular coverage. Second, the angle of the incident muons varies just between $-30°$ and $+30°$ from the vertical axis due to the geometrical acceptance of the detector system. This is limiting the vertical resolution.

In addition to all the features present in the concrete slab, an additional high-density vertical band is present towards the left edge of all the muon tomography images. This is the

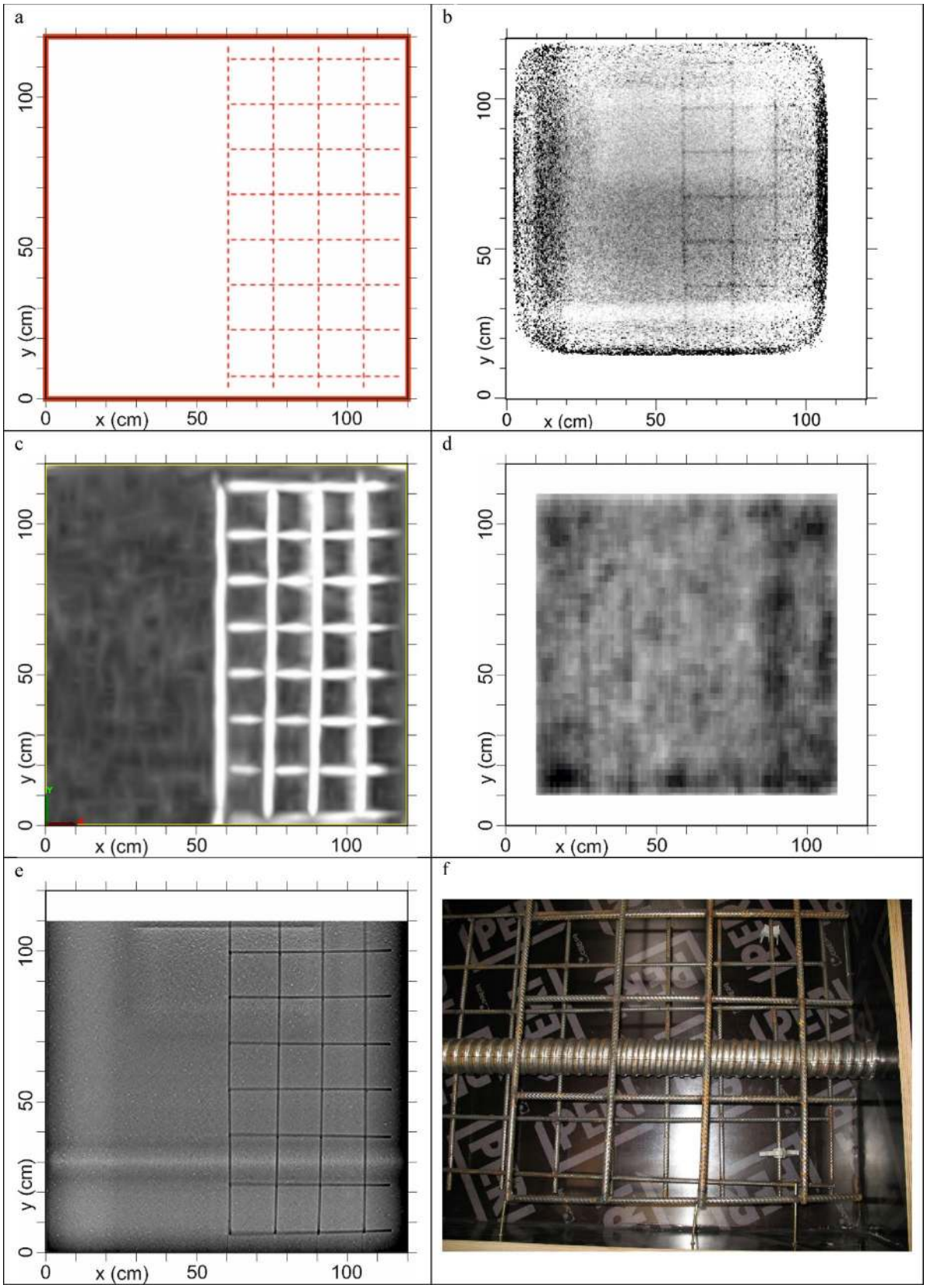

Fig. 6 The horizontal cross-sections, depth of 5 cm (upper reinforcement). **a** Design with upper reinforcement, **b** muon tomography, **c** radar, **d** ultrasound (y-Polarization), **e** X-ray laminography and **f** detail of upper reinforcement (slightly irregular mesh)

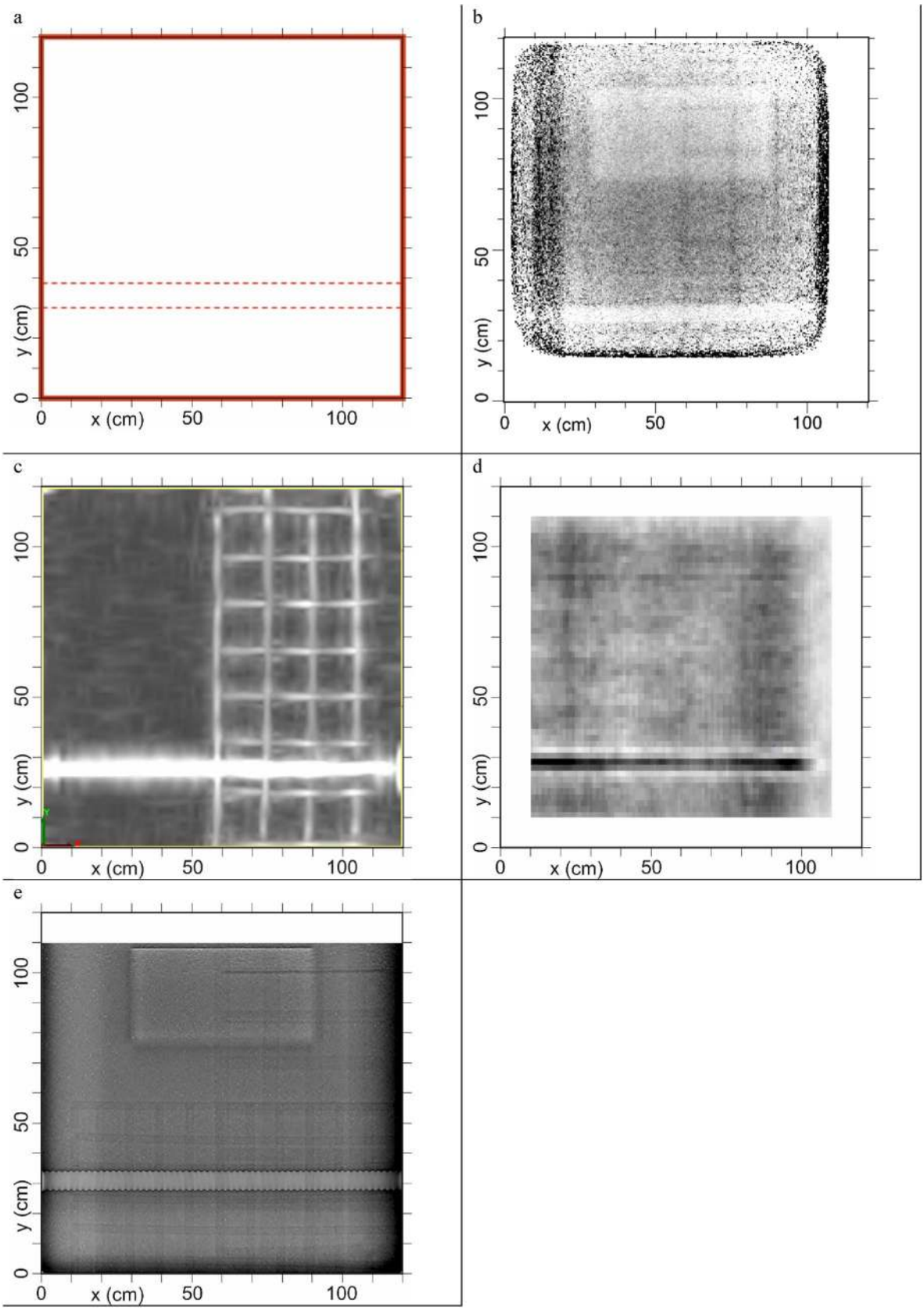

Fig. 7 The horizontal cross-sections, depth of 12 cm (tendon duct). **a** design with position of tendon duct, **b** muon tomography, **c** radar, **d** ultrasound (x-polarization) and **e** X-ray laminography

shadow of part of the support structure which held the concrete sample in position during the measurement. The image edges are noisier and more sensitive to misalignment due to the limited acceptance of events only from vertical muons.

The comparison of muon tomography images with those of X-ray laminography show similarities (shadowing effects from above and below, edge effects, different signature of low- and high-density objects). The resolution of the images as well as the low noise level are distinct advantages of active X-ray technologies. Still, the quality of the muon tomography images is even in this early stage (first-ever experiment on reinforced concrete using a new technology in a non-optimized setup) fully sufficient for an assessment of the internal geometry of the object under investigation, e. g. for deriving positions where it is safe to drill.

The distortions of the reinforcement grid in the NDT images compared to the design drawings was shown to be due to actual misalignment of some rebars. This hints to the capability of these techniques, including muon tomography, to provide detailed, high resolution checks of the actual position of features compared to the design in practical applications. However, the degree of accuracy must be determined in further research.

5 Conclusion and Outlook

Our first-ever experiment with muon tomography of a reinforced concrete block was successful. All built-in features were detected and correctly identified. The clarity of the images matches the one of radar and ultrasound while the resolution might even be better. The detection limit for rebar is smaller than 1 cm diameter rebar. However, a thorough quantitative assessment and validation of the results is still pending. Note, that the data shown here required a recording time in the order of weeks while the acquisition of ultrasonic data was performed within about two hours and of the radar data in less than 30 min. Equipment costs and requirements regarding operator skills are currently much lower for radar and ultrasound as well. Muon tomography in its current state does not reach the image quality of X-ray tomography. However, it does not require any radiation safety measures on site.

We are optimistic that muon tomography can be developed into a useful tool for non-destructive structural investigations to fill the gaps in technologies currently used on site. The highest priority to progress this exciting technology is the development of an efficient and affordable mobile muon detector, which could be mounted above and below bridge decks or inside and outside of box girders. Measurement and processing parameters still must be optimized. A thorough validation of the technology and its possibilities and limitations has to follow. We foresee that a combination of different technologies using methods from data fusion and/or improvements of the reconstruction software using machine leaning will be important steps on the way to becoming a standard technology.

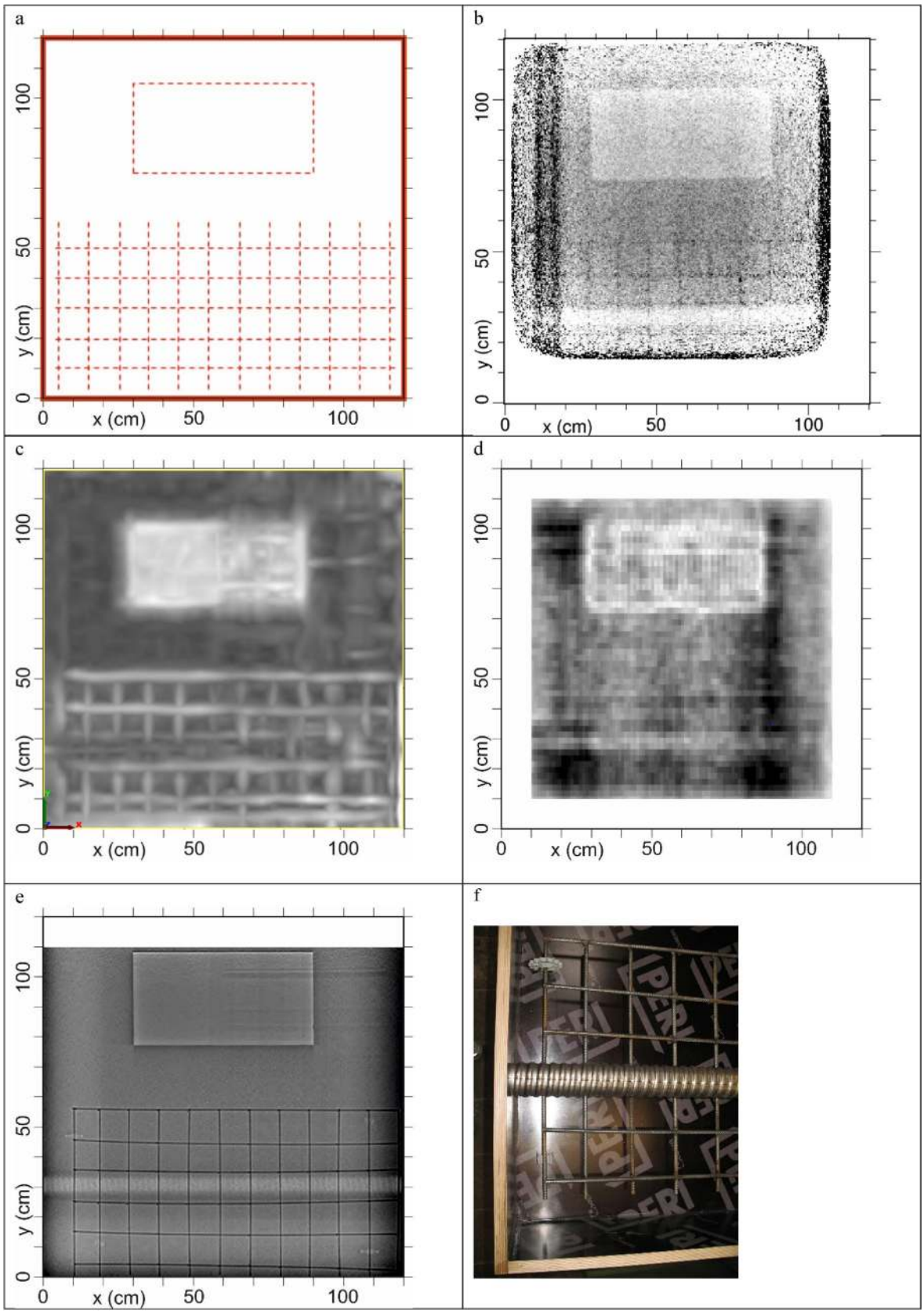
a
b
c
d
e
f
y (cm)
x (cm)
0
50
100

◂**Fig. 8** The horizontal cross-sections, depth of 17 cm (lower reinforcement and Styrofoam plate). **a** design with position of reinforcement and Styrofoam plate, **b** muon tomography, **c** radar, **d** ultrasound (y-Polarization), **e** X-ray laminography and **f** detail of lower reinforcement (distance between leftmost bars in y-direction smaller than usual)

Acknowledgements The work of the University of Glasgow has been supported by funding from STFC and EPSRC via the University of Glasgow Impact Accelerator Account.

Funding Open Access funding enabled and organized by Projekt DEAL.

Data Availability The data are available from the authors on request. The reference concrete block is accessible at BAM.

Code Availability No special code has been developed for this study.

Declarations

Conflict of interest The authors state no conflict of interests.

References

1. European Union Road Federation: Road Asset Management – An ERF position paper for maintaining and improving and efficient road network. http://erf.be/wp-content/uploads/2018/07/Road-Asset-Management-for-web-site.pdf (2018). Accessed 10 July 2020
2. German Road Research Institute (BASt): Bridge Statistics. https://www.bast.de/BASt_2017/DE/Statistik/Bruecken/Brueckenstatistik.pdf (2020). Accessed 10 July 2020.
3. Patrick, C., Dadgert, M.: Sécurité des ponts: éviter un drame. Rapport d'information fait au nom de la commission de l'aménagement du territoire et du développement durable no. 609 (2018–2019), https://www.senat.fr/notice-rapport/2018/r18-609-notice.html (2019). Accessed 8 Feb 2021.
4. Breysse, D. (ed.): Non-Destructive Assessment of Concrete Structures: Reliability and Limits of Single and Combined Techniques; State-of the Art Report of the RILEM Technical Committee 207-INR. RILEM State-of-the-Art Reports. Springer, Dordrecht (2012)
5. Helmerich, R., Niederleithinger, E., Algernon, D., Streicher, D., Wiggenhauser, H.: Bridge inspection and condition assessment in Europe. Transp. Res. Record **2044**(1), 31–38 (2008). https://doi.org/10.3141/2044-04
6. Maierhofer, C., Reinhardt, H.W., Dobmann, G. (eds.): Non-destructive Evaluation of Reinforced Concrete Structures. Vol. 1: Deterioration Processes and Standard Test Methods. CRC Press/Woodhead, Boca Raton (2010)
7. Buyukozturk, O. (ed.): Nondestructive Testing of Materials and Structures: Proceedings of NDTMS-11, Istanbul, Turkey, May 15–18, 2011. RILEM Bookseries, v. 6. Springer, Dordrecht (2013)
8. Balayssac, J.P., Garnier, V. (eds.): Non-destructive Testing and Evaluation of Civil Engineering Structures. Structures Durability in Civil Engineering Set. ISTE Press/Elsevier, London (2018)
9. Kaiser, R.: Muography: Overview and future directions. Philos. Trans. R. Soc. A **377**(2137), 20180049 (2019). https://doi.org/10.1098/rsta.2018.0049
10. Yang, G., Clarkson, T., Gardner, S., Ireland, D., Kaiser, R., Mahon, D., Al Jebali, R., Shearer, C., Ryan, M.: Novel muon imaging techniques. Philos. Trans. R. Soc. A **377**(2137), 20180062 (2019). https://doi.org/10.1098/rsta.2018.0062
11. George, E.P.: Cosmic rays measure overburden of tunnel. Commonwealth Engineer, July 1, 455–457 (1955).
12. Tanaka, H., Nagamine, K., Kawamura, N., Nakamura, S.N., Ishida, K., Shimomura, K.: Development of the cosmic-ray muon detection system for probing internal-structure of a volcano. Hyperfine Interact. **138**, 521–526 (2001). https://doi.org/10.1023/A:1020843100008
13. Mahon, D., Clarkson, A., Gardner, S., Ireland, D., Al Jebali, R., Kaiser, R., Ryan, M., Shearer, C., Yang, G.: First-of-a-kind muography for nuclear waste characterization. Philos. Trans. R. Soc. A **377**(2137), 20180048 (2019). https://doi.org/10.1098/rsta.2018.0048
14. Simpson, A., Clarkson, A., Gardner, S., Al Jebali, R., Kaiser, R., Mahon, D., Roe, J., Ryan, M., Shearer, C., Yang, G.: Muon tomography for the analysis of in-container vitrified products. Appl. Radiat. Isot. **157**, 109033 (2020). https://doi.org/10.1016/j.apradiso.2019.109033
15. Morishima, K., Kuno, M., Nishio, A., Kitagawa, N., Manabe, Y., Moto, M., Takasaki, F., et al.: Discovery of a big void in khufu's pyramid by observation of cosmic-ray muons. Nature **552**(7685), 386–390 (2017). https://doi.org/10.1038/nature24647
16. Baccani, G., Bonechi, L., Bongi, M., Casagli, N., Ciaranfi, R., Ciulli, V., D'Alessandro, R., et al.: The reliability of muography applied in the detection of the animal burrows within river levees validated by means of geophysical techniques. J. Appl. Geophys. **191**, 104376 (2021). https://doi.org/10.1016/j.jappgeo.2021.104376
17. Clarkson, A., Hamilton, D.J., Hoek, M., Ireland, D.G., Johnstone, J.R., Kaiser, R., Keri, T., et al.: Characterising encapsulated nuclear waste using cosmic-ray muon tomography. J. Instrum. **10**(3), P03020–P03020 (2015). https://doi.org/10.1088/1748-0221/10/03/P03020
18. Durham, J.M., Guardincerri, E., Morris, C.L., Bacon, J., Fabritius, J., Fellows, S., Poulson, D., Plaud-Ramos, K., Renshaw, J.: Tests of cosmic ray radiography for power industry applications. AIP Adv. **5**(6), 067111 (2015). https://doi.org/10.1063/1.4922006
19. Dobrowolska, M., Velthuis, J., Kopp, A., Perry, M., Pearson, P.: Towards an application of muon scattering tomography as a technique for detecting rebars in concrete. Smart Mater. Struct. **29**(5), 055015 (2020). https://doi.org/10.1088/1361-665X/ab7a3f
20. Zenoni A, et al.: Historical building stability monitoring by means of a cosmic ray tracking system. Proc. of the 4th Int. Conf. on Advancements in Nuclear Instrument Measurement Methods and their Applications. ANIMMA 2015, 20–24 April 2015 Lisbon: IEEE. https://arxiv.org/pdf/1403.1709.pdf (2014).
21. Vanini, S., Calvini, P., Checchia, P., Rigoni Garola, A., Klinger, J., Zumerle, G., Bonomi, G., Zenoni, D.A.: Muography of different

structures using muon scattering and absorption algorithms. Philos. Trans. R. Soc. A **377**(2137), 20180051 (2019). https://doi.org/10.1098/rsta.2018.0051
22. Schultz, L.: Cosmic ray muon radiography. Dissertation, Portland State University, Portland, OR, USA (2003)
23. Schultz, L.J., et al.: Statistical reconstruction for cosmic ray muon tomography. IEEE Trans. Image Process. **16**(8), 1985–1993 (2007). https://doi.org/10.1109/TIP.2007.901239
24. Daniels, D.J.: Ground Penetrating Radar. Institution of Engineering and Technology, London (2004)
25. Jol, H.M.: Ground Penetrating Radar: Theory and Applications. Elsevier, Amsterdam (2008)
26. Hugenschmidt, J., Kalogeropoulos, A., Soldovieri, F., Prisco, G.: Processing strategies for high-resolution GPR Concrete Inspections. NDT E Int. **43**(4), 334–342 (2010). https://doi.org/10.1016/j.ndteint.2010.02.002
27. Lai, W.L., Dérobert, X.: A review of ground penetrating radar application in civil engineering: A 30-year journey from locating and testing to imaging and diagnosis. NDT E Int. **96**, 58–78 (2018). https://doi.org/10.1016/j.ndteint.2017.04.002
28. Krause, M., Mayer, K., Friese, M., Milmann, B., Mielentz, F., Ballier, G.: Progress in ultrasonic tendon duct imaging. Eur. J. Environ. Civil Eng. **15**(4), 461–485 (2011). https://doi.org/10.1080/19648189.2011.9693341
29. Wiggenhauser, H., Samokrutov, A.A., Mayer, K., Krause, M., Alekhin, S., Elkin, V.: LAUS – Large aperture ultrasonic system for testing thick concrete structures. In: Int. Symp. Non-Destructive Testing in Civil Engineering (NDT-CE), Berlin, 15 – 17.09.2015. Berlin, Bundesanstalt für Materialforschung und –prüfung (BAM), 2015, 743–746. https://doi.org/10.1061/(ASCE)IS.1943-555X.0000314 (2015)
30. Krause, M.: Ultrasonic echo – physical principals and theory. In: Breysse, D. (ed.) Non-Destructive Assessment of Concrete Structures: Reliability and Limits of Single and Combined Techniques State-of-the-Art Report of the RILEM Technical Committee 207-INR, pp. 27–39. Springer, New York (2012)
31. Mayer, K., Cinta, P.M.: User Guide of Graphical User Interface inter_saft. University of Kassel, Department of Computational Electronics and Photonics (2012)
32. Moosavi, R., Grunwald, M., Redmer, B.: Crack detection in reinforced concrete. NDT and E Int. **109**, 102190 (2020). https://doi.org/10.1016/j.ndteint.2019.102190